



## A Measurement of the Fraction of Longitudinally-Polarized $W$ Bosons Produced in Top-Quark Decays in 200 pb $^{-1}$ of $p\bar{p}$ Collisions at $\sqrt{s} = 1.96$ TeV

The CDF Collaboration  
URL <http://www-cdf.fnal.gov>  
(Dated: July 6, 2004)

We measure the fraction of longitudinally-polarized  $W$  bosons produced in top-quark decays by analyzing the charged-lepton  $p_T$  spectrum of  $t\bar{t}$  candidate events. We find that the fraction of  $W$  bosons with longitudinal polarization is  $F_0 = 0.88^{+0.12}_{-0.47}$  (stat. + syst.),  $F_0 > 0.24$  @ 95% CL in the lepton plus jets SECVTX tagged sample;  $F_0 < 0.52$  @ 95% CL,  $F_0 < 0.94$  @ 99% CL in the dilepton sample; and  $F_0 = 0.27^{+0.35}_{-0.21}$  (stat. + syst.),  $F_0 < 0.88$  @ 95% CL in the combined analysis. The Standard Model prediction, given a top-quark mass of 175 GeV, is  $F_0 = 0.703$ .

*Preliminary Results for Summer 2004 Conferences*

## I. INTRODUCTION

This note describes a direct measurement of the fraction of longitudinally-polarized  $W$  bosons produced in top-quark decays. Given the  $V$ – $A$  form of the weak interaction, the top quark produces either a left-handed or a longitudinally-polarized  $W$  boson. Due to its large mass, decays of the top quark to longitudinally-polarized  $W$ 's are enhanced,

$$F_0 \equiv \frac{\Gamma(t \rightarrow W_0 b)}{\Gamma(t \rightarrow W_0 b) + \Gamma(t \rightarrow W_T b)} = \frac{\frac{1}{2}(m_t/m_W)^2}{1 + \frac{1}{2}(m_t/m_W)^2}. \quad (1)$$

Assuming  $m_t = 175$  GeV and  $m_b = 0$ , the Standard Model (SM) tree-level prediction is  $F_0 = 0.703$ . Decays to right-handed  $W$ 's are suppressed; at tree-level, assuming  $m_t = 175$  GeV and  $m_b = 0$ , the SM prediction is  $F_+ = 0$ .

Charged leptons from the decay of left-handed  $W$ 's are emitted in a direction opposite the line of flight of the  $W$ , giving rise to a relatively soft  $p_T$  distribution in the laboratory frame. Leptons from the decay of longitudinally-polarized  $W$ 's are emitted transverse to the line of flight of the  $W$ , giving rise to a harder  $p_T$  spectrum. We measure  $F_0$  by analyzing the charged-lepton  $p_T$  spectrum of  $t\bar{t}$  candidate events isolated in  $200 \text{ pb}^{-1}$  of  $p\bar{p}$  collisions at  $\sqrt{s} = 1.96$  TeV. These events were collected with the CDF II detector at the Fermilab Tevatron; the CDF II detector is described in detail elsewhere [1].

## II. DATA SAMPLES & EVENT SELECTION

In the SM, more than 99% of top-quark decays proceed via  $t \rightarrow Wb$ . We consider two decay channels for  $t\bar{t}$  events: the lepton plus jets channel, where one  $W$  decays leptonically and the other hadronically; and the dilepton channel, where both  $W$ 's decay leptonically.

### A. The Lepton Plus Jets Samples

The signature for  $t\bar{t}$  decay in the lepton plus jets channel consists of a single isolated charged lepton with  $p_T > 20$  GeV; three or more jets, each with  $|\eta| < 2$  and  $E_T > 15$  GeV; and missing energy in the transverse plane,  $\cancel{E}_T > 20$  GeV. This selection includes significant backgrounds due to electroweak and QCD processes. To reduce these we require that one or more jets have a displaced secondary vertex (SECVTX) tag, indicating it is consistent with the decay of a long-lived  $b$  hadron.

The total integrated luminosity for the lepton plus jets sample is  $161.6 \text{ pb}^{-1}$ . We partition the lepton plus jets data into eight disjoint samples; for each sub-sample we construct probability density functions (PDFs) of charged-lepton  $p_T$  to model the signal and the overall background. Descriptions of these samples, their event yields, and estimates of the backgrounds for each are given in table I.

Number of SECVTX Tags	1 tag				$\geq 2$ tags				$\geq 1$ tag
Primary Lepton Type	electron		muon		electron		muon		inclusive
Jet Multiplicity	3 jets	$\geq 4$ jets	3 jets	$\geq 4$ jets	3 jets	$\geq 4$ jets	3 jets	$\geq 4$ jets	$\geq 3$ jets
QCD background	$3.9 \pm 1.5$	$1.3 \pm 0.5$	$1.1 \pm 0.6$	$0.4 \pm 0.2$	$0.00 \pm 0.00$	$0.00 \pm 0.00$	$0.00 \pm 0.00$	$0.00 \pm 0.00$	$6.7 \pm 1.7$
single top background	$0.6 \pm 0.1$	$0.1 \pm 0.0$	$0.5 \pm 0.1$	$0.1 \pm 0.0$	$0.08 \pm 0.04$	$0.02 \pm 0.01$	$0.06 \pm 0.04$	$0.02 \pm 0.01$	$1.48 \pm 0.15$
$WW/WZ$ background	$0.3 \pm 0.1$	$0.1 \pm 0.0$	$0.3 \pm 0.1$	$0.0 \pm 0.0$	$0.01 \pm 0.01$	$0.01 \pm 0.01$	$0.01 \pm 0.01$	$0.00 \pm 0.01$	$0.73 \pm 0.14$
mistag background	$2.9 \pm 0.7$	$0.8 \pm 0.3$	$1.7 \pm 0.3$	$0.5 \pm 0.1$	$0.04 \pm 0.01$	$0.01 \pm 0.00$	$0.01 \pm 0.00$	$0.00 \pm 0.00$	$5.96 \pm 0.82$
$Wb\bar{b}$ background	$1.7 \pm 0.6$	$0.4 \pm 0.2$	$1.2 \pm 0.4$	$0.2 \pm 0.1$	$0.23 \pm 0.08$	$0.04 \pm 0.02$	$0.16 \pm 0.05$	$0.03 \pm 0.01$	$3.96 \pm 0.76$
$Wc\bar{c}$ background	$0.7 \pm 0.3$	$0.2 \pm 0.1$	$0.5 \pm 0.2$	$0.1 \pm 0.0$	$0.02 \pm 0.01$	$0.01 \pm 0.00$	$0.01 \pm 0.00$	$0.00 \pm 0.00$	$1.54 \pm 0.37$
$Wc$ background	$0.9 \pm 0.3$	$0.1 \pm 0.1$	$0.6 \pm 0.2$	$0.1 \pm 0.0$	$0.00 \pm 0.00$	$0.00 \pm 0.00$	$0.00 \pm 0.00$	$0.00 \pm 0.00$	$1.7 \pm 0.37$
total background	$11.1 \pm 2.0$	$2.9 \pm 0.6$	$5.7 \pm 1.0$	$1.4 \pm 0.3$	$0.39 \pm 0.10$	$0.08 \pm 0.03$	$0.25 \pm 0.07$	$0.05 \pm 0.02$	$21.9 \pm 2.3$
events observed	17	13	9	10	2	3	1	2	57

TABLE I: Sample composition estimates and event yields for the  $161.6 \text{ pb}^{-1}$  lepton plus jets samples. All uncertainties include statistical and systematic errors.

## B. The Dilepton Samples

The signature for  $t\bar{t}$  decay in the dilepton channel consists of two oppositely-charged isolated leptons, each with  $p_T > 20$  GeV; two or more jets, each with  $|\eta| < 2$  and  $E_T > 15$  GeV; and missing energy in the transverse plane,  $\cancel{E}_T > 20$  GeV.  $H_T$ , the scalar sum of energy in the transverse plane, is required to be greater than 200 GeV. This selection gives little background contamination, therefore no SECVTX tag is required.

The total integrated for the dilepton sample is  $193 \text{ pb}^{-1}$ . We partition the dilepton data into three disjoint sub-samples. For each sub-sample we construct PDFs of charged-lepton  $p_T$  to model the signal and the overall background. Descriptions of these samples, their event yields and estimates of the backgrounds for each are given in table II.

event type	$ee$	$\mu\mu$	$e\mu$	$\ell\ell$
$WW/WZ$ background	$0.21 \pm 0.06$	$0.18 \pm 0.05$	$0.34 \pm 0.10$	$0.74 \pm 0.21$
Drell-Yan background	$0.36 \pm 0.28$	$0.07 \pm 0.34$	$0.00 \pm 0.00$	$0.43 \pm 0.44$
$Z \rightarrow \tau\tau$	$0.09 \pm 0.03$	$0.11 \pm 0.03$	$0.22 \pm 0.07$	$0.42 \pm 0.13$
fake background	$0.26 \pm 0.11$	$0.16 \pm 0.07$	$0.69 \pm 0.28$	$1.1 \pm 0.45$
total background	$0.9 \pm 0.4$	$0.5 \pm 0.1$	$1.3 \pm 0.3$	$2.7 \pm 0.7$
observed	1	3	9	13

TABLE II: Sample composition estimates and event yields for the  $193 \text{ pb}^{-1}$  dilepton samples. All uncertainties include statistical and systematic errors.

## III. METHOD

We measure the fraction of longitudinal  $W$  bosons produced in top-quark decays by analyzing the charged-lepton  $p_T$  distributions of the  $t\bar{t}$  samples. We employ the method of maximum-likelihood; we construct unbinned likelihood functions composed of the charged-lepton  $p_T$  data and probability density functions (PDFs) of charged-lepton  $p_T$  representing the modeled signal and background components of these samples. The fraction of longitudinal  $W$ 's is a parameter of these functions; our estimates of  $F_0$  are those values  $\hat{F}_0$  which maximize their respective likelihood functions.

The true fraction  $F_0$  is defined within  $[0, 1]$ . However, as a parameter of the likelihood function we do not restrict  $F_0$  to this range. In order to make a coherent statement about  $F_0$  we employ the method of Feldman and Cousins [2] which always produces confidence intervals (CIs) within the defined range.

### A. The Likelihood Function

We construct an unbinned likelihood function,

$$\mathcal{L} = \prod_{s=1}^S G(\beta_s; \mu_s, \sigma_s) \prod_{i=1}^{N_s} P_s(x_i; F_0, \beta_s). \quad (2)$$

Here the first product is over the number of samples,  $S$ . The second product is over the number of reconstructed charged-leptons in sample  $s$ ,  $N_s$ . The term  $G(\beta_s; \mu_s, \sigma_s)$  is a Gaussian constraint on  $\beta_s$ , the fraction of events due to background processes in sample  $s$ . The mean  $\mu_s$  and width  $\sigma_s$  of the constraint term describe an *a priori* estimate of the background content of the sample. The term  $P_s(x_i; F_0, \beta_s)$  is the conditional probability density for sample  $s$  of charged-leptons with  $p_T = x_i$  given  $F_0$  and  $\beta_s$ . In this analysis we assume the fraction of right-handed  $W$ 's from top decays is zero<sup>1</sup>.

The per-charged-lepton probability density is

$$P_s(x_i; F_0, \beta_s) / \epsilon_s(x_i) = \beta_s P_s(x_i; \text{b.g.}) + (1 - \beta_s) [F_{0,s}^{\text{obs}}(F_0) P_s(x_i; h=0) + (1 - F_{0,s}^{\text{obs}}(F_0)) P_s(x_i; h=-1)]. \quad (3)$$

---

<sup>1</sup> This is consistent with data from CLEO on  $b \rightarrow s\gamma$  decays, which indirectly constrain the  $V+A$  charged-current coupling of the top quark [3].

$P_s(x_i; \text{b.g.})$  is the PDF for sample  $s$  of reconstructed charged-leptons with  $p_T = x_i$  due to background processes.  $P_s(x_i; h = -1)$  and  $P_s(x_i; h = 0)$  are the PDFs for sample  $s$  of reconstructed charged-leptons with  $p_T = x_i$  from the decay chain  $t \rightarrow Wb$ ,  $W \rightarrow \ell\nu_\ell$ , where the  $W$  has helicity  $h = -1$  or  $h = 0$ , respectively.

The functions  $F_{0,s}^{\text{obs}}(F_0)$  in Eq. 3 serve to correct the bias on  $F_0$  imposed by the event selection requirements. For all samples we require that reconstructed charged-leptons have  $p_T \geq 20$  GeV. Charged-leptons from left-handed  $W$ 's have a softer  $p_T$  distribution than charged-leptons from longitudinal  $W$ 's. Thus the  $p_T$  requirement biases our samples to higher average  $W$  helicity. The correction functions are parametrized by the relative acceptances of the individual sub-samples.

We correct for inefficiency in the trigger by weighting the per-charged-lepton probability density by  $\epsilon_s(x_i)$ , the expected efficiency to trigger on such a lepton. In dilepton events where both leptons are consistent with the event triggers, we apply the appropriate corrections to each lepton. We use the parametrization of the L3\_CEM.18 trigger efficiency as a function of electron  $E_T$  to weight CEM electrons. We use the parametrization of the MET\_PEM trigger efficiency as a function of electron  $E_T$  to weight triggered plug electrons in the dilepton sample. We apply no correction for the MUON\_CMUP18 and MUON\_CMX18 triggers, as there is no apparent  $p_T$  dependence for muons with track  $p_T > 20$  GeV.

#### IV. SIGNAL AND BACKGROUND MODELS

To model the signal in the lepton plus jets and dilepton samples, we use inclusive  $t\bar{t}$  samples generated with the HERWIG Monte Carlo program [4]. These are generated such that either the positively- or negatively-charged  $W$  in these events has left-handed or longitudinal polarization. The other  $W$  is polarized according to the standard model expectation.

We apply either the lepton plus jets or dilepton event selection to these samples to produce histograms of charged-lepton  $p_T$  which we use to derive the signal PDFs of Eq. 3. We impose the additional requirement that the reconstructed charged-lepton which enters these histograms be matched within a cone of  $\Delta R = 0.1$  to an electron or muon at generator-level whose parent is either the  $W$  whose helicity was fixed, or a  $\tau$  whose parent is the  $W$  whose helicity was fixed.

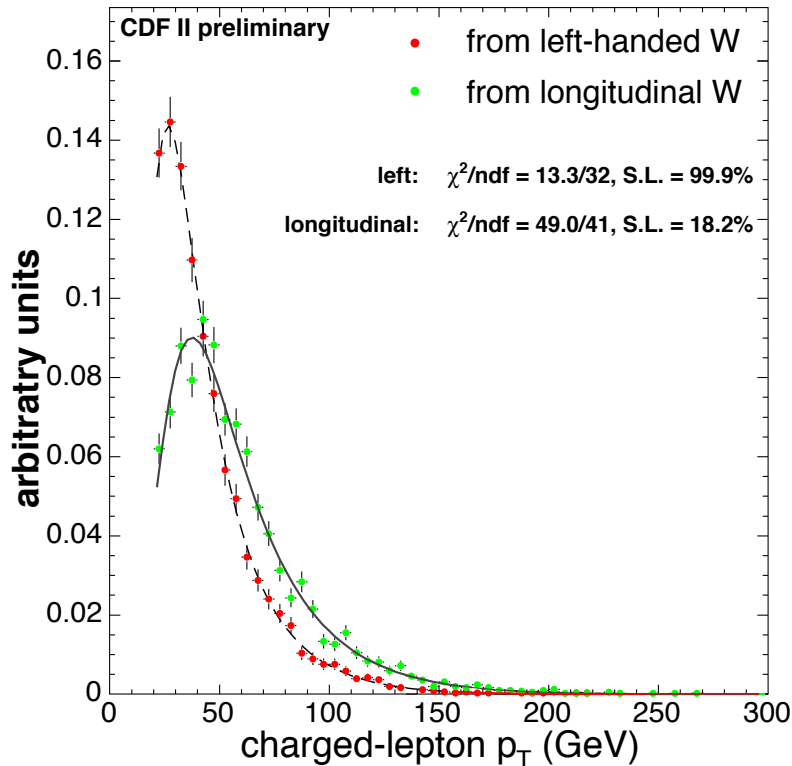


FIG. 1: Parametrization of the signal components.

The signal parametrizations are statistically indistinguishable for all the lepton plus jets and dilepton sub-samples. We use the parametrization of the inclusive lepton plus jets sample as a generic model of the signal components. This parametrization is shown in figure 1.

We compose models of the overall background as a function of charged-lepton  $p_T$  for each sub-sample by assembling histograms representing the contribution of each physics process to our acceptance according to the relative normalizations presented in tables I and II. We fit the resulting distributions to a simple analytic form.

For the lepton plus jets samples, all but the QCD background is modeled with Monte Carlo. We model the QCD background using lepton plus jets events from  $p\bar{p}$  collisions where the primary charged-lepton is non-isolated. For the dilepton samples all but the fake background is modeled with Monte Carlo. We model the fake dilepton background using dilepton events from  $p\bar{p}$  collisions where a single charged-lepton and a jet which *could* fake a charged-lepton are required.

## V. CONFIDENCE INTERVAL ESTIMATION

Our estimates of  $F_0$  are those values  $\hat{F}_0$  which maximize their respective likelihood functions; we call these Maximum Likelihood Estimators (MLEs). Since we do not restrict  $F_0$  (as a parameter of the likelihood function) to  $[0, 1]$ , we can have outcomes where the MLE is outside of the physically allowed region. We apply the method of Feldman and Cousins so that we may make a coherent statement about  $F_0$  given all possible measurement outcomes.

To construct confidence belts according to the Feldman Cousins method, it is necessary to develop an understanding of experimental resolution and bias for all possible values of the parameter to be measured. We establish this understanding by casting many ensemble tests, each consistent with our expected sample size and background composition. For these tests we allow the true parameter  $F_0$  to vary uniformly between 0 and 1 and generate events accordingly. We fit these pseudo-data according to the procedure described above to obtain the MLE  $\hat{F}_0$  for each pseudo-experiment. We observe that the distribution of MLEs is Gaussian for constant  $F_0$ . We construct parametrizations of the mean and width of the distribution of MLEs as a function of the true parameter, *i.e.*  $\mu(F_0)$  and  $\sigma(F_0)$ . We assemble these to form the resolution function

$$P(\hat{F}_0; F_0) = G(\hat{F}_0; \mu(F_0), \sigma(F_0)). \quad (4)$$

### A. Estimates of Systematic Uncertainty

We incorporate systematic uncertainties with the Feldman Cousins method by modifying the resolution function such that the statistical uncertainty  $\sigma(F_0)$  is added in quadrature with our estimate of the overall systematic uncertainty  $\sigma_{\text{sys.}}$ ,

$$P(\hat{F}_0; F_0) = G(\hat{F}_0; \mu(F_0), \sqrt{\sigma^2(F_0) + \sigma_{\text{sys.}}^2}). \quad (5)$$

Systematic uncertainties on this measurement arise from two basic sources: uncertainties inherent to the model of the signal, and uncertainties inherent to the model of the background. The former include all of the usual uncertainties that affect, for instance, the  $t\bar{t}$  acceptance. The latter include uncertainties on estimates of the rates of various contributions to the background, and uncertainties in modeling of the charged-lepton  $p_T$  distributions of each background component.

All systematic uncertainties are determined via ensemble tests. We carry out a procedure similar to the one used to estimate the resolution functions, described in section V. However, for these cases we alter the probability density functions used to generate the pseudo-data by varying each uncertain aspect of our model within those uncertainties. We then fit the varied pseudo-data using our default signal and background models. We compare the mean of the distribution of measured  $\hat{F}_0$  for the modified ensembles with the mean from the default ensemble; we take the maximum separation in means as the systematic due to the uncertainty on the varied parameter. We take the quadrature sum of each variation to be our total estimate of systematic uncertainty. Our estimates of systematic uncertainty for measurements of  $F_0$  are summarized in table III.

## VI. RESULTS

We apply the parameter estimation procedure described in section III to the data. We first consider the lepton plus jets and dilepton samples separately. We then find the value  $\hat{F}_0$  which maximizes the joint dilepton and lepton plus jets likelihood.

Source	$\sigma_{\text{syst.}} (l+\text{jets})$	$\sigma_{\text{syst.}} (\text{dileptons})$	$\sigma_{\text{syst.}} (\text{combined})$
bg normalization	0.11	0.04	0.10
top mass uncertainty	0.09	0.12	0.11
ISR/FSR	0.04	0.06	0.05
PDF uncertainty	0.03	0.04	0.03
shape uncertainty	0.03	0.02	0.02
MC statistics	0.01	0.01	0.01
acceptance correction	0.01	0.03	0.02
trigger correction	0.01	0.02	0.02
total	0.17	0.16	0.17

TABLE III: Estimates of systematic uncertainty.

### A. Result From the Lepton Plus Jets Samples

Here the likelihood function includes only the eight lepton plus jets sub-samples. Using MIGRAD we find the MLE for this sample,  $\hat{F}_0 = 0.88$ . Figure 2 shows the projection of  $-\log(\mathcal{L})$  along the  $F_0$  axis, where the background fractions for each sub-sample are fixed to those values which minimize  $-\log(\mathcal{L})$  when  $F_0 = 0.88$ . Figure 2 also shows the distribution of charged-lepton  $p_T$  data for the eight lepton plus jets samples overlaid with the total signal and background PDFs normalized according to their MLEs.

We construct Feldman Cousins confidence belts at the 68.3%, 95.4% and 99.7% confidence levels. These belts are shown in figure 2, along with MLE for this measurement. From this construction we find  $F_0 = 0.88^{+0.12}_{-0.47}$  (stat. + syst.) and  $F_0 > 0.24$  @ 95% CL in the lepton plus jets only measurement. This result is consistent with the SM prediction.

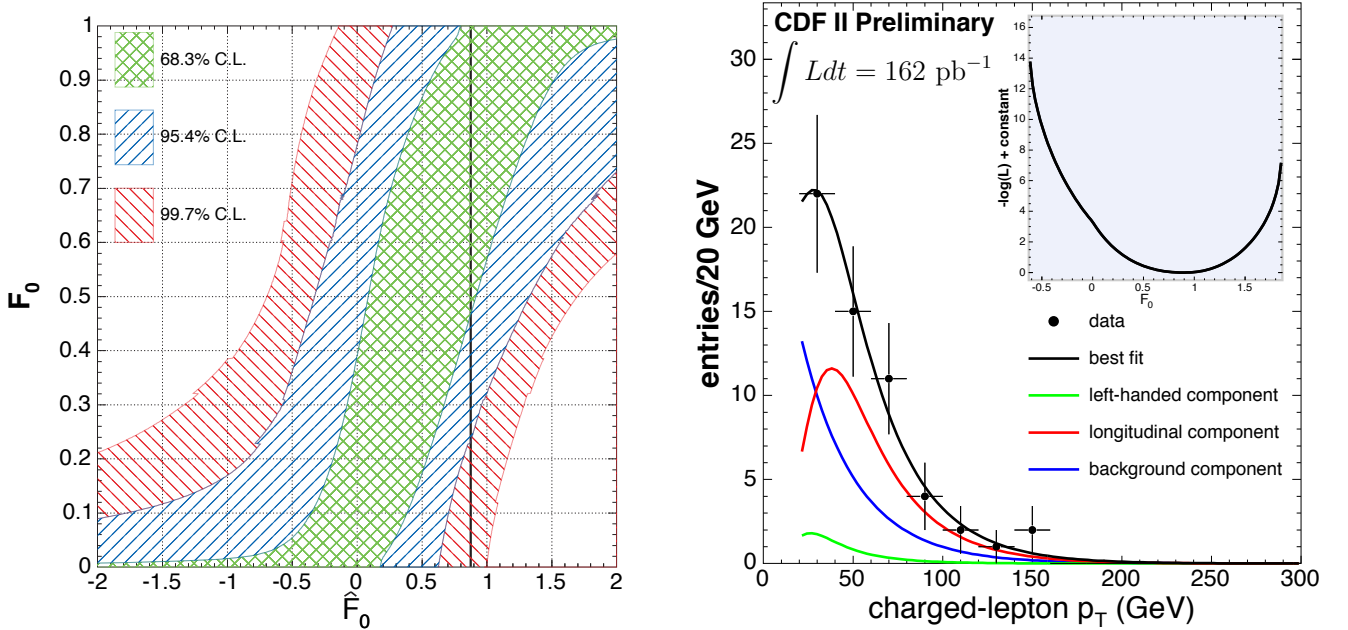


FIG. 2: Left: 1, 2 and  $3\sigma$  Feldman Cousins confidence belts for an experiment including the lepton + jets samples. These belts include systematic uncertainties. The thick vertical line indicates the experimental outcome,  $\hat{F}_0 = 0.88$ . Right: The distribution of charged-lepton  $p_T$  for the lepton plus jets samples overlaid with the total signal and background PDFs normalized according to their MLEs. Inset is the projection of  $-\log(\mathcal{L})$  along the  $F_0$  axis for the fit to the lepton + jets samples only. The background fractions are fixed to the values which absolutely maximize the likelihood function.

## B. Result From the Dilepton Samples

Here the likelihood function includes only the three dilepton sub-samples. Using MIGRAD, we find the MLE for this sample,  $\hat{F}_0 = -0.54$ . Figure 3 shows the projection of  $-\log(\mathcal{L})$  along the  $F_0$  axis, where the background fractions for each sub-sample are fixed to those values which minimize  $-\log(\mathcal{L})$  when  $F_0 = -0.54$ . Figure 3 also shows the distribution of charged-lepton  $p_T$  data for the three dilepton samples overlaid with the total signal and background PDFs normalized according to their MLEs. In this case, the distribution of charged-lepton  $p_T$  from the data is *softer* than any component of the signal or background in our model. As a consequence, the longitudinal component, which has a harder  $p_T$  distribution than the left-handed component, is forced to be negative to fit the data. However, we can make a statement about the true value of  $F_0$  by applying the Feldman Cousins method.

We construct Feldman Cousins confidence belts at the 68.3%, 95.4% and 99.7% confidence levels. These belts are shown in figure 3, along with MLE for this measurement. From this construction we find  $F_0 < 0.52$  @ 95% CL, and  $F_0 < 0.94$  @ 99% CL in the dilepton only measurement.

The dilepton data is inconsistent with the standard model prediction  $F_0 = 0.70$  at the 1 and  $2\sigma$  levels. However, the dilepton data is consistent with the lepton plus jets data at the  $2\sigma$  level. Given this level of agreement, it is reasonable to assume that we observe the same physical process in both samples. Because of this level of agreement, and because it was our *a priori* to measure  $F_0$  in the combined samples, we do so.

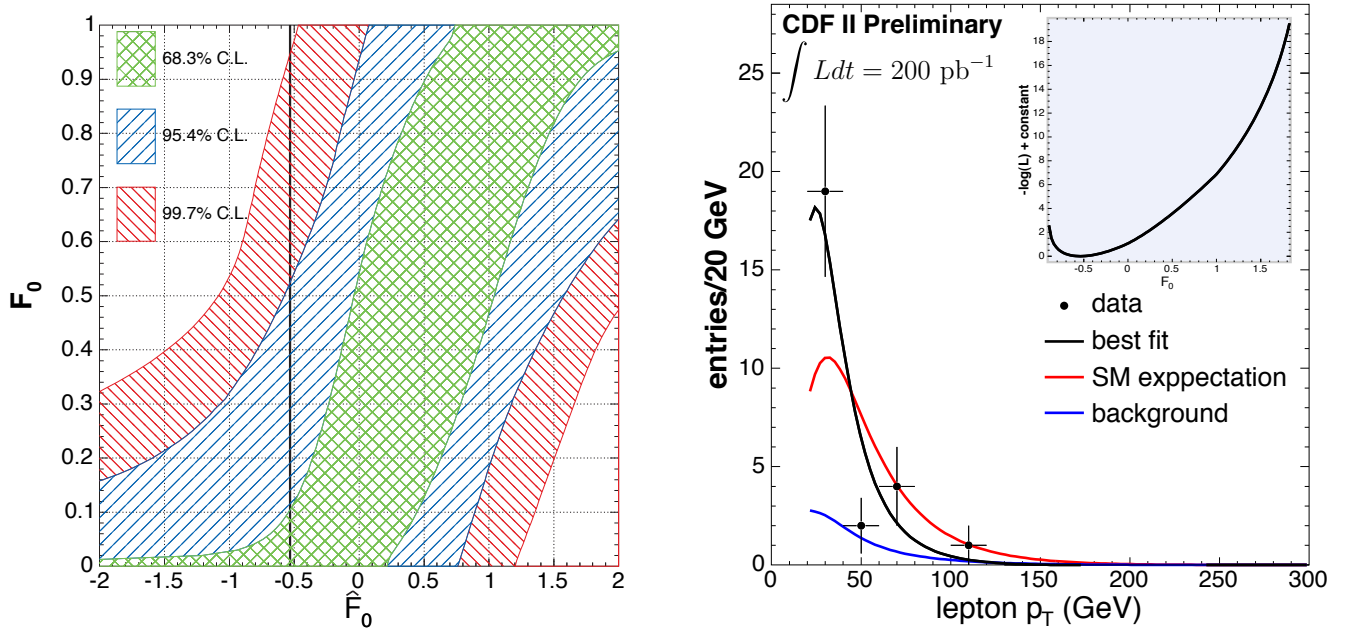


FIG. 3: Left: 1, 2 and  $3\sigma$  Feldman Cousins confidence belts for an experiment including the dilepton samples. These belts include systematic uncertainties. The thick vertical line indicates the experimental outcome,  $\hat{F}_0 = -0.54$ . Right: The distribution of charged-lepton  $p_T$  for the dilepton samples overlaid with the total signal and background PDFs normalized according to their MLEs as well as the Standard Model expectation for this sample. Inset is the projection of  $-\log(\mathcal{L})$  along the  $F_0$  axis for the fit to the dilepton samples only. The background fractions are fixed to the values which absolutely maximize the likelihood function.

## C. Result From the Combined Samples

Here the likelihood function includes the three dilepton and the eight lepton plus jets sub-samples. Using MIGRAD, we find the MLE for the combined measurement,  $\hat{F}_0 = 0.27$ . Figure 4 shows the projection of  $-\log(\mathcal{L})$  along the  $F_0$  axis, where the background fractions for each sub-sample are fixed to those values which minimize  $-\log(\mathcal{L})$  when  $F_0 = 0.27$ . Figure 4 also shows the distribution of charged-lepton  $p_T$  data for the three dilepton and eight lepton+jet samples overlaid with the total signal and background PDFs normalized according to their MLEs. The MLE for the combined measurement is consistent with the  $2\sigma$  intervals from the dilepton and lepton plus jets only measurements.

We construct Feldman Cousins confidence belts at the 68.3%, 95.4% and 99.7% confidence levels. These belts are shown in figure 4, along with MLE for the combined measurement. From this construction we find  $F_0 = 0.27^{+0.35}_{-0.21}$  (stat. + syst.) and  $F_0 < 0.88$  @ 95% CL in the combined analysis. This result is inconsistent with the standard model prediction  $F_0 = 0.70$  at the  $1\sigma$  level; it is consistent with the standard model prediction at the  $2\sigma$  level.

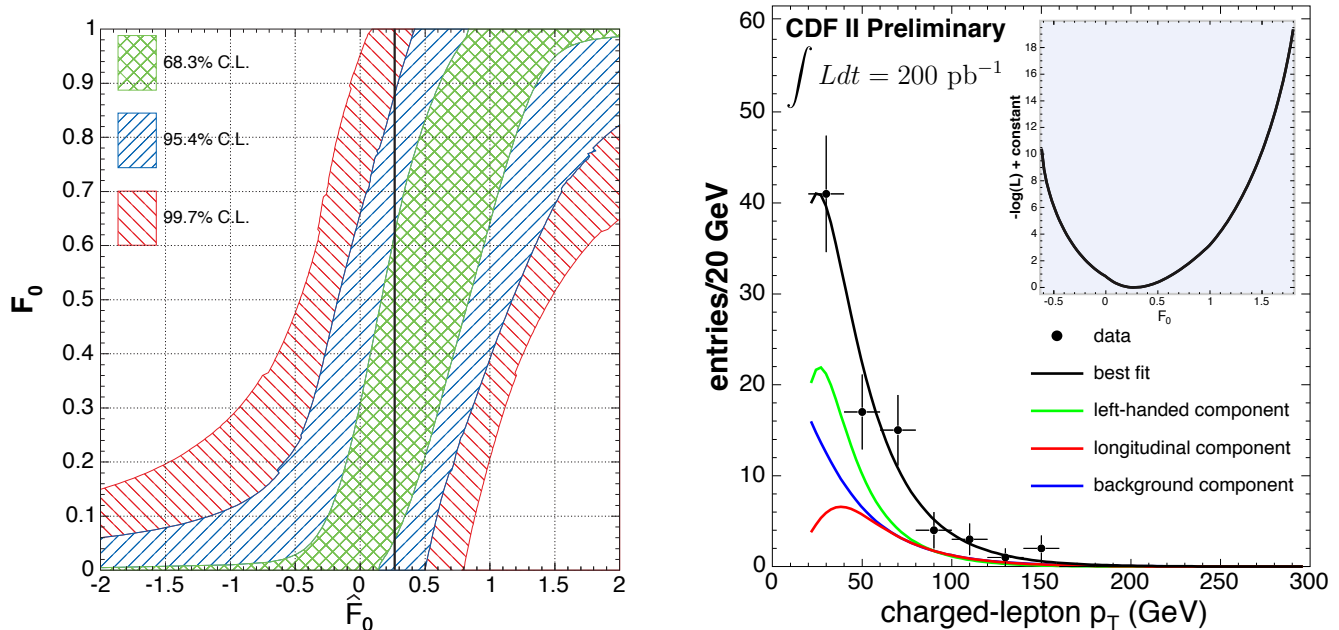


FIG. 4: Left: 1, 2 and  $3\sigma$  Feldman Cousins confidence belts for an experiment including the lepton plus jets and dilepton samples. These belts include systematic uncertainties. The thick vertical line indicates the experimental outcome,  $\hat{F}_0 = 0.27$ . Right: The distribution of charged-lepton  $p_T$  for the lepton plus jets and dilepton samples overlaid with the total signal and background PDFs normalized according to their MLEs. Inset is the projection of  $-\log(\mathcal{L})$  along the  $F_0$  axis for the fit to the lepton plus jets and dilepton samples. The background fractions are fixed to the values which absolutely maximize the likelihood function.

## VII. CONCLUSIONS

We have measured the fraction of longitudinally polarized  $W$  bosons produced in top-quark decay. The apparent disagreement between the Standard Model and the dilepton data and between the dilepton and lepton plus jets data is tantalizing. Clearly this aspect of top-quark physics bears further investigation.

In order to make a stronger statement about the nature of the  $tWb$  coupling with this method, larger statistics are required. However alternative methods, particularly the matrix-element method developed at DØ [5], should be especially powerful, even with limited statistics.

This analysis can be extended to produce a measurement of the fraction of right-handed  $W$ s produced in top-quark decay. Such a result is forthcoming.

## Acknowledgments

We thank the Fermilab staff and the technical staffs of the participating institutions for their vital contributions. This work was supported by the U.S. Department of Energy and National Science Foundation; the Italian Istituto Nazionale di Fisica Nucleare; the Ministry of Education, Culture, Sports, Science and Technology of Japan; the Natural Sciences and Engineering Research Council of Canada; the National Science Council of the Republic of China; the Swiss National Science Foundation; the A.P. Sloan Foundation; the Bundesministerium fuer Bildung und Forschung, Germany; the Korean Science and Engineering Foundation and the Korean Research Foundation; the

Particle Physics and Astronomy Research Council and the Royal Society, UK; the Russian Foundation for Basic Research; the Comision Interministerial de Ciencia y Tecnologia, Spain; and in part by the European Community's Human Potential Programme under contract HPRN-CT-20002, Probe for New Physics.

- 
- [1] F. Abe, et al., Nucl. Instrum. Methods Phys. Res. A **271**, 387 (1988); D. Amidei, et al., Nucl. Instrum. Methods Phys. Res. A **350**, 73 (1994); F. Abe, et al., Phys. Rev. D **52**, 4784 (1995); P. Azzi, et al., Nucl. Instrum. Methods Phys. Res. A **360**, 137 (1995); The CDFII Detector Technical Design Report, Fermilab-Pub-96/390-E.
  - [2] G. Feldman and R. Cousins. A Unified Approach to the Classical Statistical Analysis of Small Signals. *Phys. Rev.*, D57:3873–3889, 1998.
  - [3] K. Fujikawa and A. Yamada, “Test of the chiral structure of the top - bottom charged current by the process  $b \rightarrow s\gamma$ ,” Phys. Rev. D **49**, 5890 (1994).
  - [4] G. Corcella et al., HERWIG 6: An Event Generator for Hadron Emission Reactions with Interfering Gluons (including supersymmetric processes), JHEP **01**, 10 (2001).
  - [5] F. Canelli. Helicity of the  $W$  Boson in Single-Lepton  $t\bar{t}$  Events. FERMILAB-THESIS-2003-22.